OsteoArthritis and Cartilage (2006) **14,** 1126–1135

doi:10.1016/j.joca.2006.04.004

Osteoarthritis and Cartilage

International Cartilage Repair Society

OARSI OSTEOARTHRITIS RESEARCH SOCIETY INTERNATIONAL

Microfracture and bone morphogenetic protein 7 (BMP-7) synergistically stimulate articular cartilage repair

A. C. Kuo M.D., Ph.D.†*, J. J. Rodrigo M.D.†[a], A. H. Reddi Ph.D.†, S. Curtiss A.S.†, E. Grotkopp Ph.D.‡ and M. Chiu M.Sc.§

† *The Center for Tissue Regeneration and Repair, Department of Orthopaedic Surgery, University of California, Davis, 4635 Second Avenue, Room 2000, Sacramento, CA 95817, USA*

‡ *Section of Evolution and Ecology, University of California, Davis, 1 Shields Avenue, Davis, CA 95616, USA*

§ *Department of Pathology, University of California, Davis, 1 Shields Avenue, Davis, CA 95616, USA*

Summary

Objective: Microfracture is used to treat articular cartilage injuries, but leads to the formation of fibrocartilage rather than native hyaline articular cartilage. Since bone morphogenetic protein 7 (BMP-7) induces cartilage differentiation, we hypothesized that the addition of the morphogen would improve the repair tissue generated by microfracture. We determined the effects of these two treatments alone and in combination on the quality and quantity of repair tissue formed in a model of full-thickness articular cartilage injury in adolescent rabbits.

Design: Full-thickness defects were made in the articular cartilage of the patellar grooves of forty, 15-week-old rabbits. Eight animals were then assigned to (1) no further treatment (control), (2) microfracture, (3) BMP-7, (4) microfracture with BMP-7 in a collagen sponge (combination treatment), and (5) microfracture with a collagen sponge. Animals were sacrificed after 24 weeks at 39 weeks of age. The extent of healing was quantitated by determining the thickness and the surface area of the repair tissue. The quality of the repair tissue was determined by grading specimens using the International Cartilage Repair Society Visual Histological Assessment Scale.

Results: Compared to controls, BMP-7 alone increased the amount of repair tissue without affecting the quality of repair tissue. Microfracture improved both the quantity and surface smoothness of repair tissue. Compared to either single treatment, the combination of microfracture and BMP-7 increased both the quality and quantity of repair tissue.

Conclusions: Microfracture and BMP-7 act synergistically to stimulate cartilage repair, leading to larger amounts of repair tissue that more closely resembles native hyaline articular cartilage.

Key words: Microfracture, Cartilage, Bone morphogenetic protein 7, BMP-7.

Introduction

Injuries to articular cartilage are common, frequently lead to disability, and have a limited ability for self-repair. Lacerations to cartilage that are superficial to the tidemark do not heal, while injuries that penetrate the subchondral plate often heal with fibrocartilage[1]. The lack of repair in the former case may result from the avascular nature of cartilage, which prevents access to components of the wound healing process, including growth factors and progenitor cells. In contrast, cartilage injuries that penetrate bone lead to bleeding into the defect and the formation of a fibrin clot. This clot subsequently remodels into fibrocartilage.

Multiple surgical procedures have been developed to treat articular cartilage injuries, including marrow-stimulation techniques, autologous and allogeneic osteochondral transplantation, autologous chondrocyte implantation, and periosteal grafting[2]. In marrow-stimulation procedures, including subchondral bone microfracture, Pridie drilling, and abrasion chondroplasty, the subchondral plate at the base of a chondral defect is surgically disrupted. This leads to fibrin clot and subsequent fibrocartilage formation. Microfracture is the most well-studied marrow-stimulation procedure, and involves the arthroscopic penetration of the subchondral plate with an awl. In case series with up to 17 years of follow-up, microfracture has led to durable improvements in both patient symptoms and function[3]. Microfracture also compares favorably with other treatments. In a randomized controlled trial comparing microfracture with autologous chondrocyte implantation, both treatments led to short-term clinical improvement with microfracture leading to a significantly better improvement in the Short Form-36 (SF-36) physical component score[4].

Despite these positive clinical results, questions remain about the quality and durability of the fibrocartilage formed after microfracture. In animal models of marrow stimulation, the regenerated cartilage clearly differs from normal articular cartilage, with increased amounts of type I collagen, altered tissue architecture, and random orientation of collagen

[a] *Current address:* Steadman Hawkins Clinic of the Carolinas, 1690 Skylyn Drive, Spartanburg, SC 29307, USA.

*Address correspondence and reprint requests to: Dr. Alfred Chung Kuo, M.D., Ph.D., The Center for Tissue Regeneration and Repair, Department of Orthopaedic Surgery, University of California, Davis, 4635 Second Avenue, Room 2000, Sacramento, CA 95817, USA. Tel: 1-916-734-2807; Fax: 1-916-734-3939; E-mail: alfred.kuo@ucdmc.ucdavis.edu

Received 6 July 2005; revision accepted 4 April 2006.

fibers[5]. In addition, this repair cartilage may degenerate over time, with surface fibrillation, loss of hyaline appearance, and loss of structural integrity[6,7]. Therefore, the clinical outcomes of patients undergoing microfracture would likely be improved if more normal repair cartilage were produced.

Application of morphogenetic proteins may be one approach to enhance the repair tissue generated by microfracture[8,9]. With the proper stimulation, the mesenchymal cells in the initial fibrin clot may be induced to assume and maintain a phenotype that more closely resembles normal articular cartilage. In particular, both *in vitro* and *in vivo* experiments suggest that bone morphogenetic protein 7 (BMP-7), also known as osteogenic protein-1, may aid the healing of chondral defects. This morphogen is capable of inducing *de novo* cartilage formation and also plays a role in the maintenance of articular cartilage. It is found in normal articular cartilage[10] and stimulates chondrocyte proliferation, differentiation, and metabolism[11–16]. In addition, other BMP family members also enhance the metabolism and phenotypic maintenance of chondrocytes[17,18]. Finally, intra-articular delivery of BMP-7 using a mini-osmotic pump enhanced articular cartilage repair in a sheep model of chondral injury[19].

These results suggest that microfracture and BMP-7 treatment will synergistically enhance cartilage healing, with microfracture recruiting stem cells and BMP-7 stimulating the proliferation and chondrocytic differentiation of these cells. This may lead to a repair cartilage that is more similar to normal articular cartilage than the tissue induced by either treatment alone. Combining the two treatments may also provide a simple method for localized morphogen/growth factor delivery within a joint. Growth factor impregnated matrices can be securely press-fit into the enclosed spaces provided by microfracture holes. Diffusion of factors would then lead to high local concentrations within a chondral defect.

We have therefore examined the effects of microfracture and BMP-7 treatment, alone and in combination, on the healing of full-thickness articular cartilage lesions in adolescent rabbits.

We sought to address the following four hypotheses:

(1) Microfracture leads to improvement in the quantity and quality of repair tissue compared with control lesions.
(2) Application of soluble BMP-7 leads to improvement in the quantity and quality of repair tissue compared with control lesions.
(3) Microfracture combined with BMP-7 delivered in a collagen sponge (combination treatment) leads to improvement in the quantity and quality of repair tissue compared with microfracture alone.
(4) Microfracture combined with BMP-7 delivered in a collagen sponge (combination treatment) leads to improvement in the quantity and quality of repair tissue compared with the application of soluble BMP-7 alone.

Method

ANIMAL MODEL

All animal protocols were reviewed and approved by our Institutional Animal Care and Use Committee. Fifteen-week-old male New Zealand white rabbits weighing 2.5–3 kg were used in this study. Following intravenous administration of adequate anesthesia (50 mg/kg ketamine, 5 mg/kg xylazine, and 0.5 mg/kg acepromazine), a medial parapatellar skin incision was made in the right knee of each animal. The incision was extended through the joint capsule and the patella was subluxated laterally. A 2 mm by 7 mm full-thickness defect was made in the articular cartilage of the trochlear groove using a curette. Care was taken to minimize disruption of the underlying subchondral bone, which differed from cartilage in appearance, consistency, and resistance to curetting.

The experiment consisted of the following five treatment groups, with eight animals in each group:

Treatment 1 Control defects: no additional treatment.
Treatment 2 Microfracture: Using 18 gauge needles, two 3 mm deep microfractures were made through the subchondral bone at the base of the defect, one proximally and one distally. Each microfracture hole was 1.5 mm in diameter and the holes were separated by 2 mm.
Treatment 3 BMP-7: 10 μg of recombinant human BMP-7 (Stryker Corporation, Hopkinton, MA) dissolved in 10 μl of 5 mM hydrochloric acid was painted onto the bone at the base of the chondral lesion and allowed to adsorb for 5 min.
Treatment 4 Microfracture plus BMP-7 adsorbed onto a collagen sponge (combination treatment): After microfracture, 10 μg of BMP-7 dissolved in 10 μl of 5 mM hydrochloric acid was adsorbed onto a 2 mm diameter by 3 mm tall cylinder of a type I collagen sponge (Helistat Sponge, Integra LifeSciences, Plainsboro, NJ) for 15 min. This sponge was then press-fit into the distal microfracture hole.
Treatment 5 Microfracture plus collagen sponge: After microfracture, a 2 mm diameter by 3 mm tall cylinder of type I collagen sponge soaked in 10 μl of 5 mM hydrochloric acid was press-fit into the distal microfracture hole.

Following the above treatments, magnified digital photographs of the chondral defects were taken [Fig. 1(A)]. The resolution of these photographs was comparable to the images seen using a dissecting microscope. The patellae were reduced and the wounds were closed in two layers with absorbable sutures. For pain control, the animals received 0.1 mg buprenorphine subcutaneously immediately after surgery and then daily until comfortable. Postoperative complications were recorded. The animals were not immobilized and were allowed unrestricted activity in their cages until sacrifice at 24 weeks (39 weeks of age). Gait was observed prior to sacrifice. The patellofemoral joints were then exposed, the chondral defects were photographed [Fig. 1(B)], and blocks of bone containing the trochlear grooves were excised. The contralateral, unoperated trochlear grooves were also harvested from four animals in each treatment group.

As a control for our model and in particular to confirm that the defects were full-thickness cartilage lesions, chondral defects were made in six additional knees. These samples were immediately excised, prepared for histology, and stained with hematoxylin and eosin (H&E) as described below.

QUANTITATION OF TISSUE SURFACE AREA

Photographs of the chondral defects at the time of both surgery and sacrifice were analyzed using the Scion Image image-analysis program (Scion Corp., Frederick, MD). A single, blinded observer made all measurements. The area of the defect at the time of surgery was determined (quantity *B* in Fig. 2)

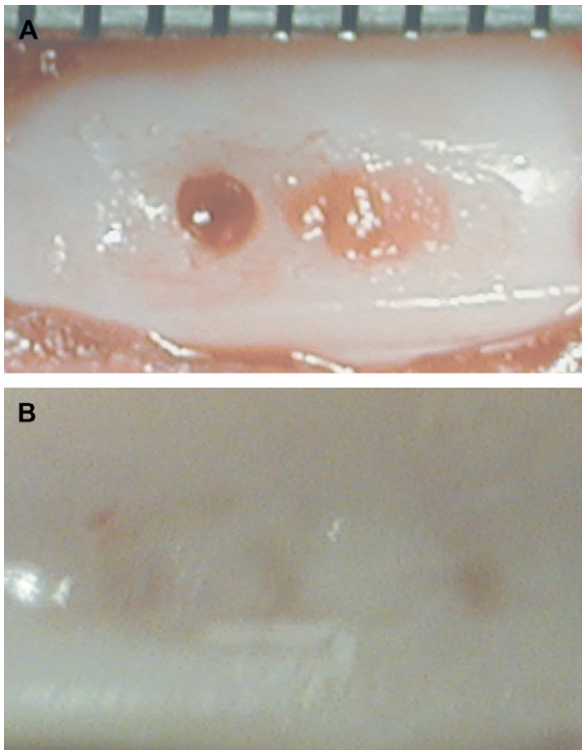

Fig. 1. Gross appearance of a chondral defect. (A) Intraoperative appearance of a chondral defect. The specimen has been treated with microfracture and a collagen sponge. The collagen sponge has been press-fit into the microfracture hole on the right. The ruler shows millimeter spacing. (B) Appearance of a chondral defect at sacrifice. The lesion shown in (A) has been filled with two large areas of repair tissue.

as well as the area of the defect at the time of sacrifice (quantity *C* in Fig. 2). These values were used to calculate the percentage of the original defect surface area covered with repair tissue at the time of sacrifice as follows (Fig. 2):

$$\text{Percentage of surface area covered} = [(B - C)/B] \times 100.$$

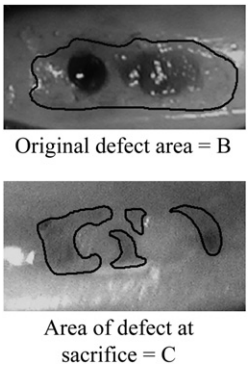

$$\text{Percentage of original defect surface area covered with repair tissue at sacrifice} = \frac{\text{Area repair tissue}}{\text{Original defect area}} \text{ X } 100 = \frac{\text{B-C}}{\text{B}} \text{ X } 100$$

Fig. 2. Calculation of the percentage of the original defect surface area covered with repair tissue at sacrifice. In order to quantitate the percentage of the original defect surface area covered with repair tissue, photographs were taken of the defects at the time of surgery (top panel) and sacrifice (bottom panel). The surface areas of the defects at surgery (*B*) and at sacrifice (*C*) were quantitated and used to calculate the percentage of surface area covered as shown.

HISTOLOGY

The trochlear grooves were fixed for 48 h in 10% neutral buffered formalin. Samples were then decalcified in 10% formic acid with 0.2 M sodium citrate. Following extensive washing in water, 2-mm-thick transverse slices across the trochlea were made. Two samples from each specimen, one from the proximal area of the defect and one from the distal region, were then dehydrated in ethanol, embedded in paraffin, and sectioned at 4 μm. These transverse sections were then stained with each of the following: (1) H&E, (2) safranin-O and fast green, (3) a monoclonal antisera against type I collagen (Ab-1; Oncogene Research Products, Boston, MA) at a 1:100 dilution, and (4) a monoclonal antisera against type II collagen (Ab-1; Oncogene Research Products, Boston, MA) at a 1:100 dilution. Immunostaining was completed using a biotinylated horse anti-mouse secondary immunoglobulin (Vector, Burlingame, CA) with the Vectastain ABC-AP reagent and Vector Red as substrate or with the Vectastain ABC-peroxidase reagent and diaminobenzidine as substrate (Vector, Burlingame, CA). Photomicrographs were taken of each tissue region using the 20× objective. Samples were visualized using both white and polarized light.

The repair tissue, adjacent normal articular cartilage, and normal cartilage from the unoperated contralateral knees were graded using the International Cartilage Repair Society (ICRS) Visual Histological Assessment Scale[20] by one blinded observer (Table I). Samples were judged to be hyaline if they had a homogenous matrix, abundant safranin-O staining, abundant type II collagen immunostaining, little or no type I collagen immunostaining, round cells in lacunae, and an organized collagen arrangement under polarized light. Fibrocartilage was defined as a sample with distinct fibers in the matrix, round or elliptical cells with or without

Table I
ICRS Visual Histological Assessment Scale

Feature	Score
I. Surface	
Smooth/continuous	3
Discontinuities/irregularities	0
II. Matrix	
Hyaline	3
Mixture: hyaline/fibrocartilage	2
Fibrocartilage	1
Fibrous tissue	0
III. Cell distribution	
Columnar	3
Mixed/columnar-clusters	2
Clusters	1
Individual cells/disorganized	0
IV. Cell population viability	
Predominantly viable	3
Partially viable	1
<10% viable	0
V. Subchondral bone	
Normal	3
Increased remodeling	2
Bone necrosis/granulation tissue	1
Detached/fracture/callus at base	0
VI. Cartilage mineralization (calcified cartilage)	
Normal	3
Abnormal/inappropriate location	0

lacunae, abundant or mildly reduced safranin-O staining, both type I and type II collagen immunostaining, and a disorganized collagen arrangement when viewed under polarized light. Mixed tissue was defined as having at least 30% hyaline cartilage, with the remainder being fibrocartilage. Fibrous tissue was defined as having a fibrous matrix with small, irregularly-shaped cells, little or no safranin-O staining, little or no type II collagen immunostaining, abundant type I collagen immunostaining, and a disorganized appearance under polarized light (Fig. 3). Repair tissue was not present on two sections from the control group and three sections from the BMP-7 single treatment group. These specimens were neither graded using the ICRS scale nor scored for tissue thickness as described below.

QUANTITATION OF TISSUE THICKNESS

Digital images of histology specimens stained with H&E and/or safranin-O were captured and then analyzed using the Scion Image image-analysis program. For each slide, the total area of repair tissue (quantity *A*, Fig. 4) was measured as well as the total length of repair tissue (quantity *L* Fig. 4). The average thickness of the repair cartilage was then defined as *A*/*L*. The average thickness of normal articular cartilage from the same slide was calculated similarly. In order to normalize these results, the percentage thickness of the repair tissue relative to the control tissue was calculated as follows:

$$\text{Percentage thickness} = [(\text{Average thickness repair tissue}) / (\text{Average thickness control tissue})] \times 100.$$

All measurements for thickness determination were made by one blinded observer.

STATISTICAL ANALYSIS

StatView 4.51 (Abacus Concepts, Berkeley, CA) was used for all statistical analyses. The values for both percentage surface area covered and percentage thickness of the repair tissue were arcsine transformed to approximate a normal distribution. To test the hypotheses for these continuous variables, analysis of variance and Fisher's protected

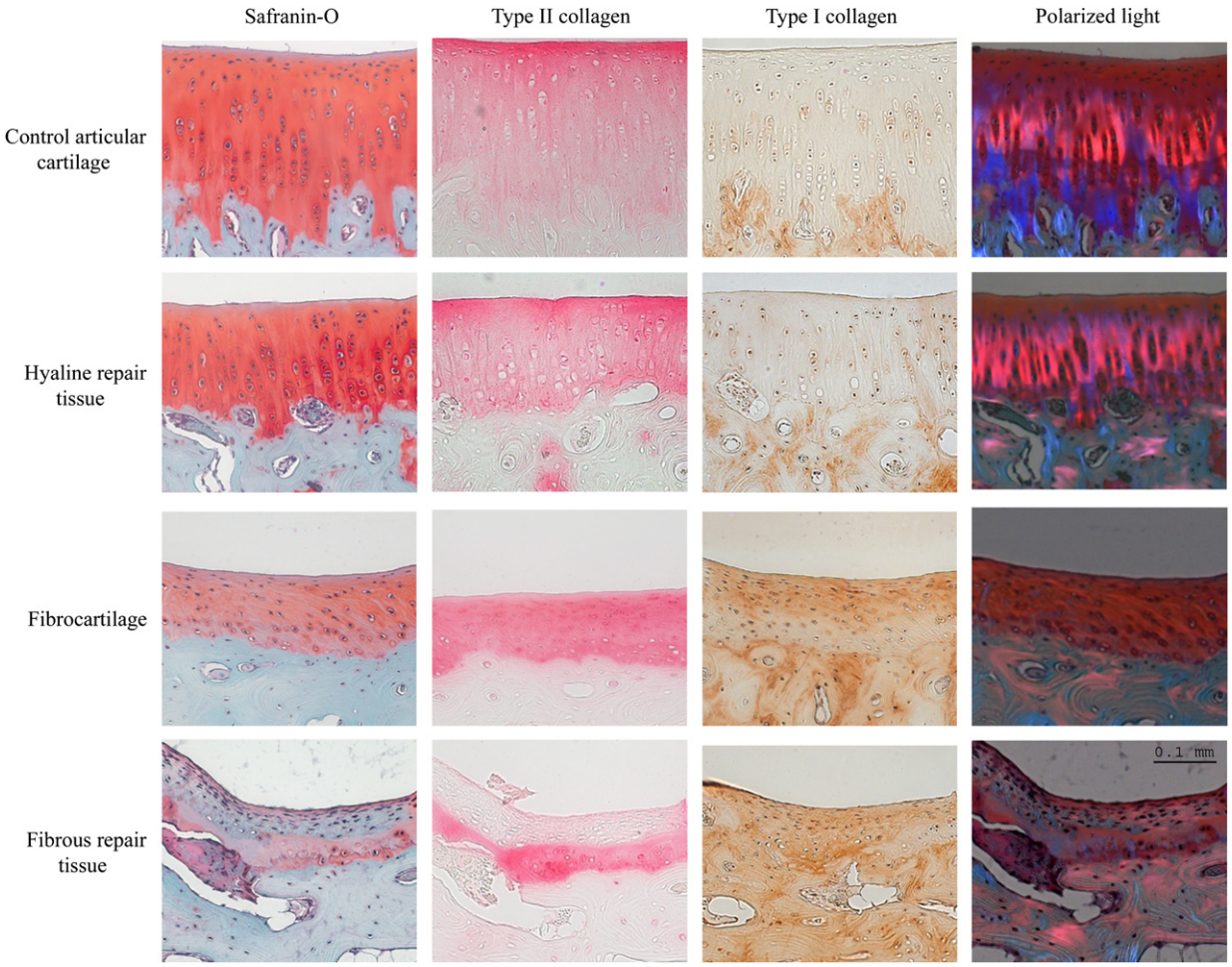

Fig. 3. Histological results. Representative specimens of normal, control articular cartilage (combination treatment group), hyaline repair tissue (combination treatment group), fibrocartilage (microfracture single treatment group), and fibrous repair tissue (control defect group) are shown. Please see text for a discussion of staining patterns. The specimens in the far left column have been stained with safranin-O and fast green and visualized with white light. The second column shows type II collagen immunostaining. The third column shows type I collagen immunostaining. The specimens in the far right column have been stained with safranin-O and fast green and visualized with polarized light. Scale is as indicated in the lower right panel (objective, 20×).

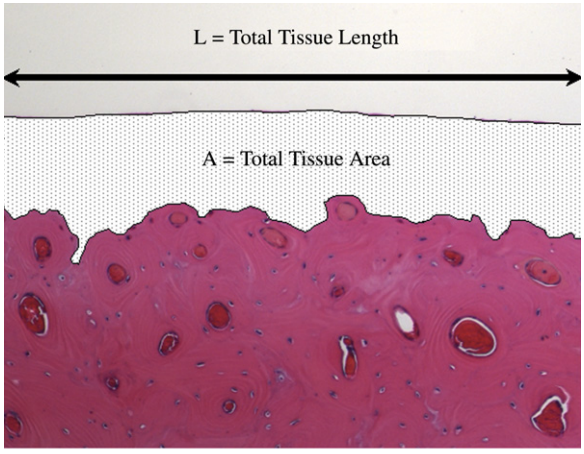

Fig. 4. Calculation of average tissue thickness. Image analysis of histology specimens was used to quantitate the average thickness of both repair tissue and normal adjacent articular cartilage. The total length of the tissue (*L*) and the total area of the tissue (dotted area *A*) were quantitated and then used to calculate average thickness as shown. Specimens were stained with H&E and viewed using the 20× objective.

least significant difference test were used to detect significantly different means among the four planned comparisons. These *P* values were then adjusted upwards by a sequential Bonferroni procedure to control the family-wise Type I error rate and reported.

For the categorical variables in the ICRS Histological Scale (surface, matrix, cell distribution, cell population viability, subchondral bone, and cartilage mineralization), contingency tables were analyzed for each hypothesis tested and Fisher's exact *P* with a correction for continuity was noted. These *P* values were then adjusted upwards by a sequential Bonferroni procedure to control the family-wise Type I error rate and reported. Although repair tissues were assessed using four categories for both matrix-type and cell distribution, it was necessary to group specimens with scores of 0 and 1 and to group specimens with scores of 2 and 3 for statistical analysis of the histology results. Specimens with scores of 2 or 3 were defined as having superior matrix/cell distribution, while specimens with scores of 0 or 1 were defined as having inferior matrix/cell distribution.

Additionally, to assess the role of the collagen sponge used in the combination treatment, comparisons were made between the combination treatment (microfracture with BMP-7 in a collagen sponge) and microfracture with a collagen sponge alone. Simple *t* tests were conducted for percentage surface area covered and percentage thickness of the repair tissue (arcsine transformed), while contingency tables were analyzed for the components of the ICRS scale.

Results

To verify that we created full-thickness articular cartilage defects, six control knees were examined histologically immediately after defect creation. In all six knees, all of the cartilage was removed except for remnants of calcified cartilage that interdigitated with the subchondral bone. There was minimal disruption of the underlying subchondral plate with no penetration of the marrow cavity [Fig. 5(A)]. The cartilage of animals at this age has the structure of adult cartilage, with a superficial zone, a radial zone, and a calcified zone with a distinct tidemark [Fig. 5(B)].

All of the experimental animals survived surgery. There were no postoperative complications. All animals ambulated normally prior to sacrifice at 24 weeks. On gross examination at the time of sacrifice, defects were filled with variable amounts of tissue similar in color, consistency, and height to the surrounding normal cartilage [Fig. 1(B)]. The histology results varied widely, with repair tissue ranging from organized hyaline tissue to disorganized fibrous tissue (Fig. 3). The undamaged articular cartilage surrounding the repair tissue was histologically identical to normal articular cartilage from the contralateral control knees with similar safranin-O staining (data not shown).

There were no differences among the treatment groups in the ICRS categories of cell population viability (all samples scored as 3, predominantly viable), subchondral bone (all samples scored as 3, normal), and cartilage mineralization (all samples scored as 3, normal). The results for each treatment for percentage surface area covered, percentage thickness of the repair tissue, and the ICRS categories of surface, matrix, and cell distribution are shown in Figs. 6–10.

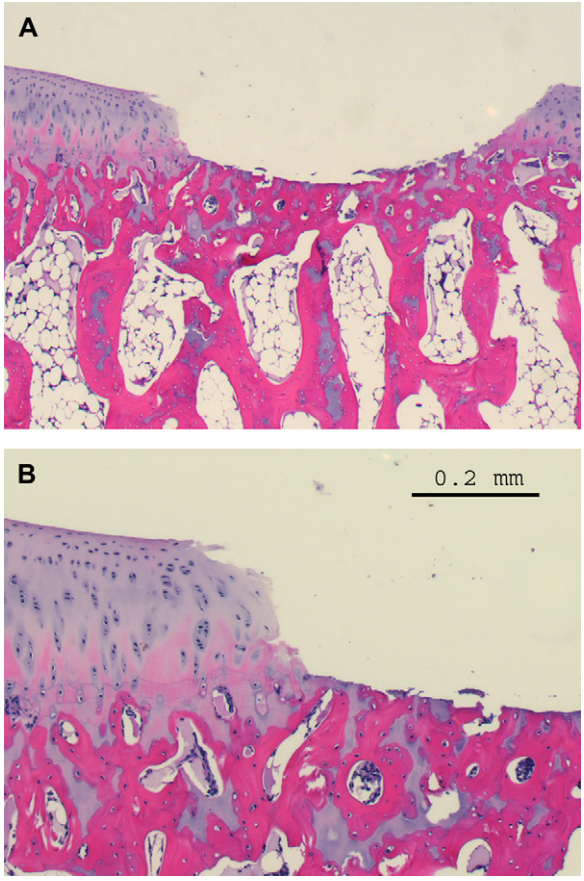

Fig. 5. Histological appearance of a chondral defect immediately after creation. (A) Low power (objective, 2.5×). (B) High power (objective, 10×). Scale is as indicated.

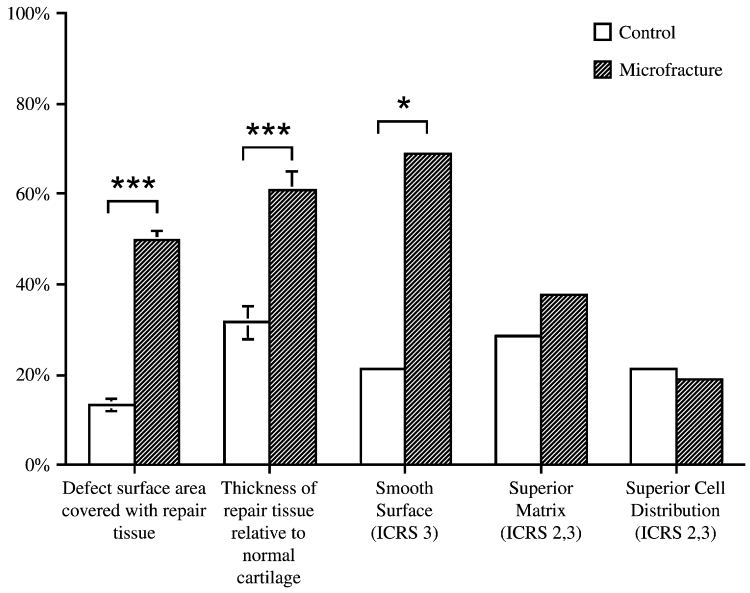

Fig. 6. Comparison of microfracture with controls (hypothesis 1). Comparison of the microfracture single treatment group and the control defect group for percentage surface area covered, percentage thickness, percentage of specimens with smooth surface (ICRS 3), percentage of specimens with superior matrix (ICRS 2 and 3), and percentage of specimens with superior cell distribution (ICRS 2 and 3). *Indicates $P < 0.05$; ***indicates $P < 0.001$.

MICROFRACTURE VS CONTROL (HYPOTHESIS 1)

Compared to controls, microfracture resulted in a statistically significant improvement in both the amount and surface smoothness of the repair tissue. There was an increase in percentage surface area covered compared with control defects (50% vs 13%, $P < 0.0003$) as well as percentage thickness (61% vs 34%, $P = 0.0005$). The microfracture group had a significantly greater proportion of samples with a smooth surface (ICRS score 3) than the control group (69% vs 21%, $P = 0.041$). There were not significant differences in the percentage of specimens with either superior matrix or superior cell distribution (Fig. 6).

BMP-7 VS CONTROL (HYPOTHESIS 2)

Compared to controls, BMP-7 resulted in a statistically significant increase in the amount of repair tissue without affecting the quality of the repair tissue. There was an increase in the percentage surface area covered compared with the control group (31% vs 13%, $P < 0.0004$), but not percentage thickness (34% vs 34%, NS). There was a trend

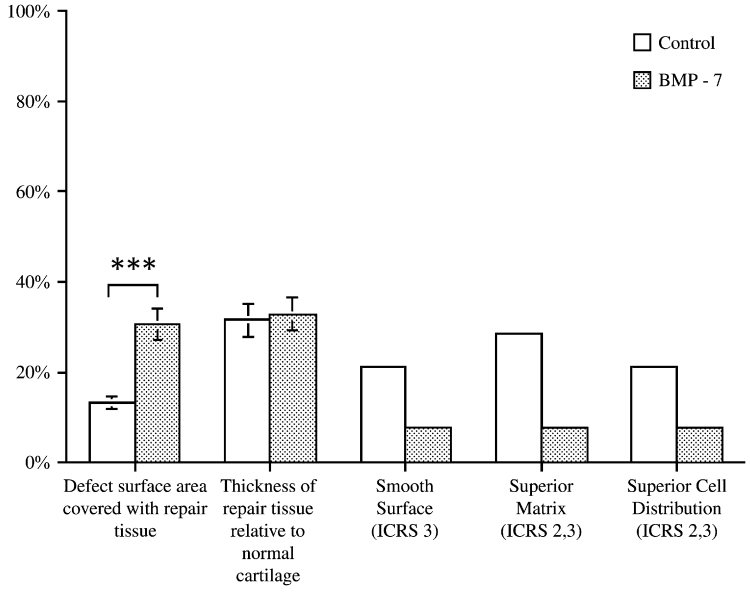

Fig. 7. Comparison of BMP-7 with controls (hypothesis 2). Comparison of the BMP-7 single treatment group and the control defect group for percentage surface area covered, percentage thickness, percentage of specimens with smooth surface (ICRS 3), percentage of specimens with superior matrix (ICRS 2 and 3), and percentage of specimens with superior cell distribution (ICRS 2 and 3). ***Indicates $P < 0.001$.

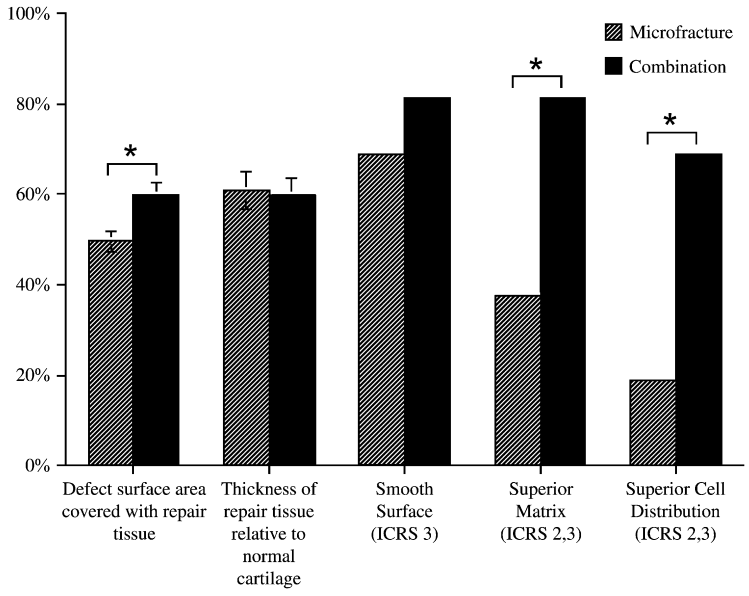

Fig. 8. Comparison of the combination treatment with microfracture (hypothesis 3). Comparison of the combination treatment group (microfracture with BMP-7 in a collagen sponge) with the microfracture single treatment group for percentage surface area covered, percentage thickness, percentage of specimens with smooth surface (ICRS 3), percentage of specimens with superior matrix (ICRS 2 and 3), and percentage of specimens with superior cell distribution (ICRS 2 and 3). *Indicates $P < 0.05$.

toward worsening surface, matrix, and cell distribution for the BMP-7 treatment group, however, these differences did not reach significance (Fig. 7).

COMBINATION OF MICROFRACTURE WITH BMP-7 IN A COLLAGEN SPONGE (COMBINATION TREATMENT) VS MICROFRACTURE ALONE (HYPOTHESIS 3)

The combination treatment induced a statistically significant improvement in both the quantity and quality of repair tissue compared with microfracture alone. There was an increase in percentage surface area covered (60% vs 50%, $P = 0.014$). The combination treatment group had the same percentage thickness as the microfracture group (60% vs 61%, NS). The combination treatment and microfracture both resulted in predominantly smooth surface (81% vs 69%, NS). The combination treatment resulted in significantly improved matrix and cell distribution compared with microfracture alone. The combination treatment resulted in significantly more samples with superior matrix

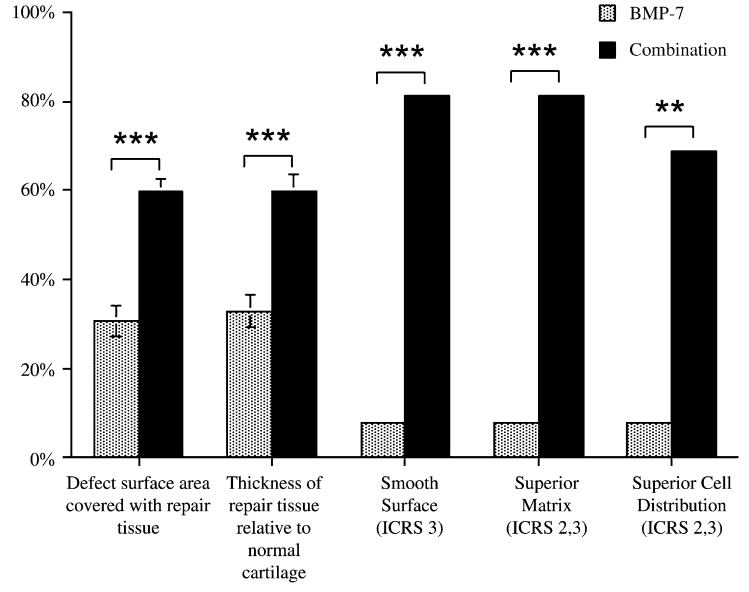

Fig. 9. Comparison of the combination treatment with BMP-7 (hypothesis 4). Comparison of the combination treatment group (microfracture with BMP-7 in a collagen sponge) with the BMP-7 single treatment group for percentage surface area covered, percentage thickness, percentage of specimens with smooth surface (ICRS 3), percentage of specimens with superior matrix (ICRS 2 and 3), and percentage of specimens with superior cell distribution (ICRS 2 and 3). **Indicates $P < 0.01$; ***indicates $P < 0.001$.

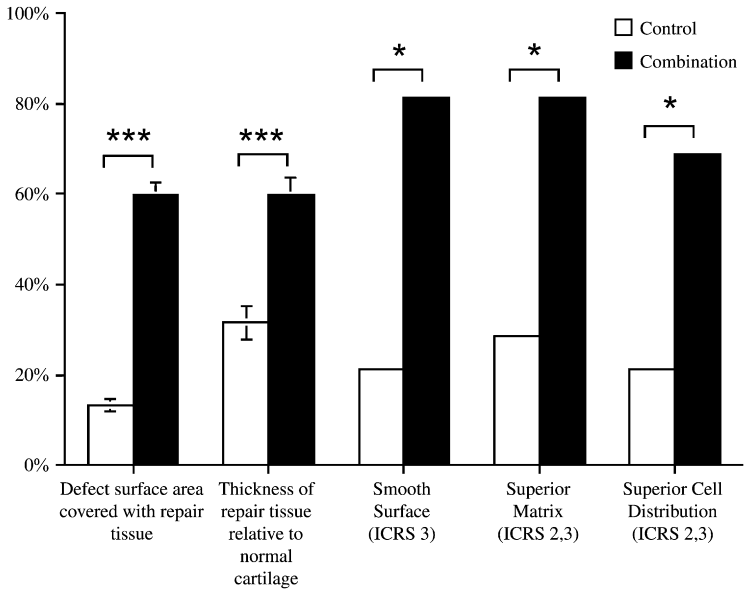

Fig. 10. Comparison of the combination treatment with controls. Comparison of the combination treatment group (microfracture with BMP-7 in a collagen sponge) with the control defect group for percentage surface area covered, percentage thickness, percentage of specimens with smooth surface (ICRS 3), percentage of specimens with superior matrix (ICRS 2 and 3), and percentage of specimens with superior cell distribution (ICRS 2 and 3). *Indicates $P < 0.05$; ***indicates $P < 0.001$.

(81% vs 38%, $P = 0.048$). Significantly more samples from the combination treatment group had superior cell distribution compared with the microfracture alone group (69% vs 19%, $P = 0.019$) (Fig. 8).

COMBINATION OF MICROFRACTURE WITH BMP-7 IN A COLLAGEN SPONGE (COMBINATION TREATMENT) VS BMP-7 ALONE (HYPOTHESIS 4)

The combination group had more and better repair tissue compared to the BMP-7 group. There was an increase in the percentage surface area covered (60% vs 31%, $P < 0.0001$), as well as the percentage thickness (60% vs 34%, $P = 0.0009$). The combination treatment also resulted in significant improvements in surface, matrix, and cell distribution. The samples with the combination treatment were predominantly smooth, while few were smooth with BMP-7 alone (81% vs 8%, $P = 0.0005$). There were significantly more samples with superior matrix for the combination treatment compared with BMP-7 alone (81% vs 8%, $P = 0.0005$). Significantly more samples receiving the combination treatment also had superior cell distribution compared with BMP-7 alone (69% vs 8%, $P = 0.009$) (Fig. 9). The combination group also had similar improvements relative to the control group (Fig. 10).

EFFECT OF THE COLLAGEN SPONGE CARRIER: COMBINATION TREATMENT VS MICROFRACTURE PLUS COLLAGEN SPONGE

In order to assess the effect of the collagen sponge used as a carrier for BMP-7, we compared the combination treatment (microfracture and BMP-7 in a collagen sponge) with microfracture plus collagen sponge alone. Both treatments had similar percentage surface area covered (60% vs 64%, NS), but the combination treatment led to thicker repair tissue (60% vs 46%, $P = 0.044$). The repair tissue was mostly smooth for both groups (81% vs 56%, NS). The combination treatment group had significantly greater proportions of superior matrix (81% vs 25%, $P = 0.0038$) and superior cell distribution (69% vs 12%, $P = 0.0032$). Therefore, the sponge carrier likely contributed to the increase in surface area of repair tissue without improving tissue thickness, matrix, or cell distribution.

Discussion

While both microfracture and BMP-7 treatment alone increased the amount of repair tissue, only the combination of treatments led to improvements in the matrix and cell distribution of the repair tissue. The repair tissue in all five treatment groups had normal cell population viability, subchondral bone, and cartilage mineralization. Both microfracture and the combination treatment improved the surface of the repair tissue. The ability of microfracture alone to improve the quantity of repair tissue without greatly affecting its quality is consistent with previous equine studies[21]. These results suggest that these two treatments act synergistically, with microfracture playing the predominant role in increasing the amount of repair tissue, and BMP-7 enhancing the quality of repair tissue relative to microfracture alone. However, despite the improvements in quantity and quality of repair tissue, the combination treatment did not lead to either complete filling of the defects or completely normal hyaline articular cartilage.

One limitation of this study is that the application of soluble BMP-7 directly to a chondral defect is not equivalent to the application of BMP-7 adsorbed onto a collagen sponge. The latter form likely has a longer duration of action[22]. Therefore, the BMP-7 single treatment group may not be the optimal control for the effects of the morphogen. This may explain the lack of improvement in the histological features in this group relative to the control defect group. We elected not to include a collagen sponge in the BMP-7 single treatment group since a sponge would probably not remain stationary within a shallow chondral defect (less

than 0.4 mm deep in this study) and would likely become a loose body in the joint. In contrast, sponges that were press-fit into microfracture holes remained securely in place even with joint movement.

The optimal method of morphogen delivery for cartilage repair is unclear. Multiple matrices have been used as carriers for soluble factors. In addition to serving as carriers, these matrices may also have biological effects. The type I collagen sponge used in this study increased the surface area of repair tissue without improving either thickness or histological characteristics. Type I collagen also has been successfully used as a carrier to deliver BMPs to osteochondral defects in animal models. BMP-2 adsorbed onto a type I collagen sponge enhanced healing of osteochondral lesions in rabbits[22], while BMP-7 combined with particulate type I collagen led to hyaline-like repair of osteochondral lesions in dogs[23]. In both of these studies, the defects extended into the subchondral bone and provided deep recesses (3 mm) that held the applied matrices. In contrast, the full-thickness chondral lesions in our model, like those commonly found clinically, are significantly shallower (less than 0.4 mm in the current study; Fig. 5). Full-thickness articular cartilage defects would not hold insoluble matrices as efficiently as deeper osteochondral defects. Microfracture allowed us to overcome this by providing focal deep pockets into which sponges could be securely press-fit. Another method for the treatment of shallow cartilage defects is the delivery of morphogens using a soluble, adherent, self-gelling carrier. For example, in miniature pigs, delivery of transforming growth factor-β1 in either a fibrin or gelatin matrix led to the filling of partial-thickness chondral defects with cartilage-like tissue[24,25]. In contrast to marrow stimulation, this treatment relies on the recruitment of mesenchymal repair cells from the synovium. The indications for and relative efficacy of these two approaches must still be determined.

The timing of morphogen administration also affects healing. In contrast to our results with a single application of soluble factor, prolonged intra-articular administration of soluble BMP-7 improved both the quality and quantity of repair tissue in a sheep model of cartilage injury[19]. The differences from our results likely represent differences in the duration of morphogen treatment. In the sheep study, a mini-osmotic pump was implanted in the distal femur and was used to deliver soluble BMP-7 into the knee over 2 weeks. This lengthy treatment may enhance the differentiation of cells as well as help them maintain their chondrocytic phenotype, thereby improving the quality of repair tissue. However, implantation of an osmotic pump has more morbidity than microfracture, and would require a second surgery for pump removal.

Another limitation of this study is that the clear histological improvements seen in the combination treatment group may not lead to improved durability, mechanical properties, or function of the repair tissue. Although the repair tissue showed few signs of degeneration at sacrifice at 24 weeks, progressive deterioration might be seen at later time points. For example, in a study of osteochondral defects in both skeletally immature and mature rabbits, degenerative changes in the repair tissue increased in both frequency and severity from 12 to 48 weeks[6]. Longer follow-up is necessary to determine the ultimate fate of the patellofemoral joints as well as of the repair tissue generated by microfracture and BMP-7.

The results of this study may not be generalizable to cartilage injuries in skeletally mature individuals, since the ability of cartilage to respond to treatments depends on the age of an individual. At the time of surgery, the animals in this study were undergoing the final stages of epiphyseal development. Their femora were approximately 95% of adult length and their articular cartilage contained a superficial tangential layer, a radial layer, a calcified zone, and a distinct tidemark (Fig. 5; Ref.[26]). Sacrifice occurred after physeal closure. A different response to microfracture and BMP-7 may occur in individuals injured and treated after physeal closure. However, in a study of osteochondral defects in rabbits, 4- to 6-month-old, skeletally immature animals exhibited a similar cellular and histological response as 7- to 12-month-old, skeletally mature animals[6].

In summary, BMP-7 enhances the effects of microfracture in adolescent rabbits, leading to an improvement in the quality and quantity of repair tissue generated. Since articular cartilage injuries appear to be increasing among skeletally immature patients[27], the addition of BMP-7 in a collagen sponge may improve the clinical outcomes of young individuals undergoing microfracture. This combined technique could be easily adopted into clinical practice, since, like microfracture alone, the combination of treatments is a technically simple procedure with low morbidity.

Acknowledgements

Support for this project was provided to A.C. Kuo by the Giannini Family Foundation and Denny Dickenson.

References

1. Mankin HJ. The response of articular cartilage to mechanical injury. J Bone Joint Surg Am 1982;64:460–6.
2. Hunziker EB. Articular cartilage repair: basic science and clinical progress. A review of the current status and prospects. Osteoarthritis Cartilage 2002;10: 432–63.
3. Steadman JR, Briggs KK, Rodrigo JJ, Kocher MS, Gill TJ, Rodkey WG. Outcomes of microfracture for traumatic chondral defects of the knee: average 11-year follow-up. Arthroscopy 2003;19:477–84.
4. Knutsen G, Engebretsen L, Ludvigsen TC, Drogset JO, Grontvedt T, Solheim E, *et al.* Autologous chondrocyte implantation compared with microfracture in the knee. A randomized trial. J Bone Joint Surg Am 2004;86: 455–64.
5. Mitchell N, Shepard N. The resurfacing of adult rabbit articular cartilage by multiple perforations through the subchondral bone. J Bone Joint Surg Am 1976;58: 230–3.
6. Shapiro F, Koide S, Glimcher MJ. Cell origin and differentiation in the repair of full-thickness defects of articular cartilage. J Bone Joint Surg Am 1993;75:532–53.
7. Menche DS, Frenkel SR, Blair B, Watnik NF, Toolan BC, Yaghoubian RS, *et al.* A comparison of abrasion burr arthroplasty and subchondral drilling in the treatment of full-thickness cartilage lesions in the rabbit. Arthroscopy 1996;12:280–6.
8. Reddi AH. Role of morphogenetic proteins in skeletal tissue engineering and regeneration. Nat Biotechnol 1998;16:247–52.
9. Reddi AH. Cartilage morphogenetic proteins: role in joint development, homeostasis and regeneration. Ann Rheum Dis 2003;62(Suppl 2):ii73–8.
10. Chubinskaya S, Merrihew C, Cs-Szabo G, Mollenhauer J, McCartney J, Rueger DC, *et al.* Human articular

chondrocytes express osteogenic protein-1. J Histochem Cytochem 2000;48:239–50.
11. Asahina I, Sampath TK, Nishimura I, Hauschka PV. Human osteogenic protein-1 induces both chondroblastic and osteoblastic differentiation of osteoprogenitor cells derived from newborn rat calvaria. J Cell Biol 1993; 123:921–33.
12. Klein-Nulend J, Louwerse RT, Heyligers IC, Wuisman PI, Semeins CM, Goei SW, *et al*. Osteogenic protein (OP-1, BMP-7) stimulates cartilage differentiation of human and goat perichondrium tissue *in vitro*. J Biomed Mater Res 1998;40:614–20.
13. Klein-Nulend J, Semeins CM, Mulder JW, Winters HA, Goei SW, Ooms ME, *et al*. Stimulation of cartilage differentiation by osteogenic protein-1 in cultures of human perichondrium. Tissue Eng 1998;4:305–13.
14. Haaijman A, D'Souza RN, Bronckers AL, Goei SW, Burger EH. OP-1 (BMP-7) affects mRNA expression of type I, II, X collagen, and matrix Gla protein in ossifying long bones *in vitro*. J Bone Miner Res 1997;12:1815–23.
15. Lietman SA, Yanagishita M, Sampath TK, Reddi AH. Stimulation of proteoglycan synthesis in explants of porcine articular cartilage by recombinant osteogenic protein-1 (bone morphogenetic protein-7). J Bone Joint Surg Am 1997;79:1132–7.
16. Nishida Y, Knudson CB, Kuettner KE, Knudson W. Osteogenic protein-1 promotes the synthesis and retention of extracellular matrix within bovine articular cartilage and chondrocyte cultures. Osteoarthritis Cartilage 2000;8:127–36.
17. Luyten FP, Yu YM, Yanagishita M, Vukicevic S, Hammonds RG, Reddi AH. Natural bovine osteogenin and recombinant bone morphogenetic protein-2B are equivalent in the maintenance of proteoglycans in bovine articular cartilage explant culture. J Biol Chem 1992;267:3691–5.
18. Luyten FP, Chen P, Paralkar V, Reddi AH. Recombinant bone morphogenetic protein-4, transforming growth factor-β1, and activin A enhance the cartilage phenotype of articular chondrocytes *in vitro*. Exp Cell Res 1994;210:224–9.
19. Jelic M, Pecina M, Haspl M, Kos J, Taylor K, Maticic D, *et al*. Regeneration of articular cartilage chondral defects by osteogenic protein-1 (bone morphogenetic protein-7) in sheep. Growth Factors 2001;19:101–13.
20. Mainil-Varlet P, Aigner T, Brittberg M, Bullough P, Hollander A, Hunziker E, *et al*. International Cartilage Repair Society. Histological assessment of cartilage repair: a report by the Histology Endpoint Committee of the International Cartilage Repair Society (ICRS). J Bone Joint Surg Am 2003; 85-A(Suppl 2):45–57.
21. Frisbie DD, Trotter GW, Powers BE, Rodkey WG, Steadman JR, Howard RD, *et al*. Arthroscopic subchondral bone plate microfracture technique augments healing of large chondral defects in the radial carpal bone and medial femoral condyle of horses. Vet Surg 1999;28:242–55.
22. Sellers RS, Zhang R, Glasson SS, Kim HD, Peluso D, D'Augusta DA, *et al*. Repair of articular cartilage defects one year after treatment with recombinant human bone morphogenetic protein-2 (rhBMP-2). J Bone Joint Surg Am 2000;82:151–60.
23. Cook SD, Patron LP, Salkeld SL, Rueger DC. Repair of articular cartilage defects with osteogenic protein-1 (BMP-7) in dogs. J Bone Joint Surg Am 2003; 85-A(Suppl 3):116–23.
24. Hunziker EB, Rosenberg LC. Repair of partial-thickness defects in articular cartilage: cell recruitment from the synovial membrane. J Bone Joint Surg Am 1996;78: 721–33.
25. Hunziker EB. Growth-factor induced healing of partial-thickness defects in adult articular cartilage. Osteoarthritis Cartilage 2001;9:22–32.
26. Rivas R, Shapiro F. Structural stages in the development of the long bones and epiphyses. A study in the New Zealand white rabbit. J Bone Joint Surg Am 2002;84:85–100.
27. Moti AW, Micheli LJ. Meniscal and articular cartilage injury in the skeletally immature knee. Instr Course Lect 2003;52:683–90.